AD-A048 844 GEORGE WASHINGTON UNIV WASHINGTON D C SCHOOL OF ENGI--ETC F/G 13/13
DYNAMIC BUCKLING OF AXISYMMETRIC SPHERICAL CAPS WITH INITIAL IM--ETC(U)
DEC 77 R KAO, N PERRONE N00014-75-C-0946

UNCLASSIFIED NL

1 OF 1
ADA048 844

END
DATE FILMED
2-78
DDC

12 B.S.

THE
GEORGE
WASHINGTON
UNIVERSITY

STUDENTS FACULTY STUDY R ESEARCH DEVELOPMENT FUT URE CAREER CREATIVITY CO MMUNITY LEADERSHIP TECH NOLOGY FRONTIE ESIGN ENGINEERING APP ENC GEORGE WASHIN NIV

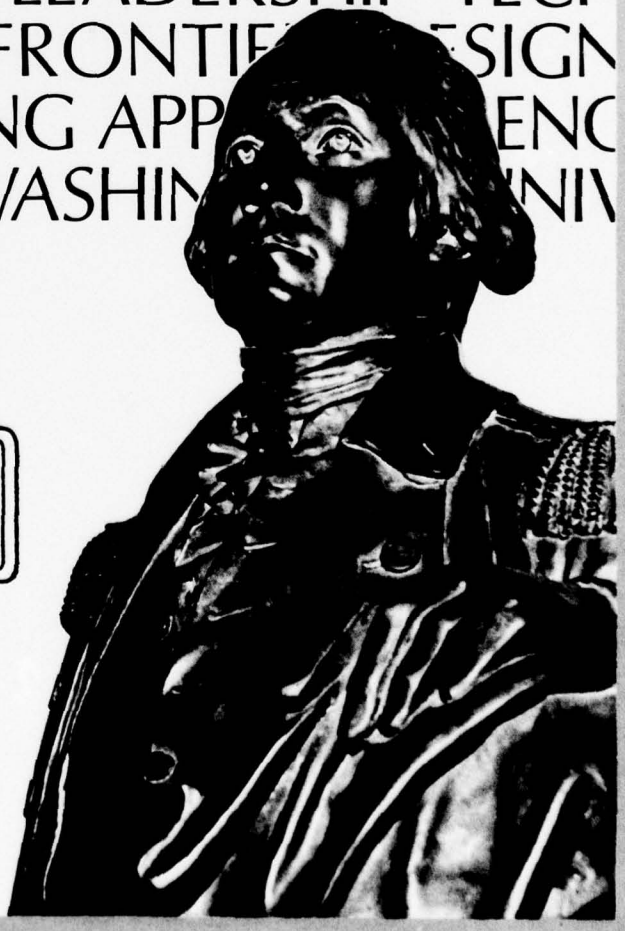

SCHOOL OF ENGINEERING
AND APPLIED SCIENCE

(12)

(6) DYNAMIC BUCKLING OF AXISYMMETRIC SPHERICAL CAPS WITH INITIAL IMPERFECTIONS,

(10) Robert/Kao and Nicholas/Perrone

Sponsored by
Office of Naval Research
Arlington, Virginia 22217

(15) Contract Number
NAVY N00014-75-C-0946

(11) December, 1977

(12) 41p.

School of Engineering and Applied Science
The George Washington University
Washington, D.C. 20052

DYNAMIC BUCKLING OF AXISYMMETRIC SPHERICAL CAPS WITH INITIAL IMPERFECTIONS[1]

By

Robert Kao[2] and Nicholas Perrone[3]

[1] The research reported on here and the first author were supported by the Office of Naval Research, Contract Number NAVYN00014-75-C-0946.

[2] Visiting Research Assistant Professor, Department of Civil, Mechanical and Environment Engineering, The George Washington University, Washington, D.C.

[3] Director of Structural Mechanics Program, Office of Naval Research, Arlington, Virginia; also, Adjunct Professor of Mechanics, The Catholic University of America, Washington, D.C.

ABSTRACT

Dynamic buckling loads are obtained for axisymmetric spherical caps with initial imperfections. Two types of loading are considered, namely, step loading with infinite duration and right triangular pulse. Solutions of perfect spherical caps under step loading are in excellent agreement with previous findings. Results show that initial imperfections do indeed have the effect of reducing the buckling capacity for both dynamic and static responses, although they are affected in a different manner. From the solutions obtained for triangular pulse situations, it is revealed that pulse duration has a very significant impact on the magnitude of the dynamic buckling load. When comparing these solutions with those of step loading, it is concluded that the step loading with infinite duration is the limiting case of a triangular pulse, and that the step loading provides the most severe loading situation for dynamic analysis.

INTRODUCTION

Dynamic buckling analysis of shell structures has received considerable attention in the literature. Shell structures designed according to quasi-static analysis may fail under conditions of dynamic loading. It is also found that initial imperfections in spherical shell structures have the effect of reducing shell static buckling capacity (Refs. [1,2,3,4]).* Initial imperfection of shell structures, in fact, is sometimes used to account for the discrepancy between results obtained from experimental tests and theorectical analyses.

The problem of axisymmetric dynamic snap-through of clamped spherical caps under implusive loading was first solved by Humphrey and Bodner [5]. The same problem under instantaneously applied step loading was studied by Budiansky and Roth [6] and Simitses [7]. Rayleigh-Ritz or Galerkin methods were used for shell dynamic buckling analysis in those studies. Archer and Lange [8] discussed the same problem numerically by solving governing differential equations by a combination of finite-difference technique and Potter method. Lock, Okubo and Whittier [9] approached this problem by performing experiments for a particular shell geometry.

The same problem under a uniform step pressure is solved numerically in Refs. [10-14] and results obtained from these investigations are in reasonable agreement. From this agreement, it may be said that the axisymmetric dynamic buckling criterion - dynamic snap-through - suggested by Budiansky and Roth [6] has generally been accepted.

Asymmetric dynamic buckling analysis of spherically caps is examined in Refs. [13,15] in which a perturbation approach was utilized to deal with asymmetric deformation mode.

---

* Numbers in brackets designate references at end of paper.

Effect of initial imperfections on static shell buckling analysis was studied by Hutchinson [1] who employed the Koiter approach to determine the approximate asymmetric buckling load for spherical shells with initial imperfections. Koga and Hoff [2] gave the values of buckling pressure for complete shells with axisymmetric dimple type imperfections. Numerical solutions for asymmetric buckling loads are given in Refs. [3,4] for spherical caps with initial asymmetric imperfections.

In this paper, attention is focused on the effect of initial imperfections on the dynamic buckling of axisymmetric spherical caps. The influence of different types of dynamic pulse shape on shell buckling capacity is also considered.

In the next section, the governing equations and solution methods utilized in the present paper are discussed. This is followed by a description of dynamic buckling criteria. To verify the present approach, a comparison of the present results with those in the literature is given for axisymmetric buckling loads of spherical caps under uniform step pressure and with initial imperfections of different magnitude. Also presented are the solutions associated with a triangular pulse with different time durations. Conclusions and a general discussion are given in the final section.

GOVERNING EQUATIONS

The geometry of a clamped spherical cap is shown in Fig. 1, in which H is the central height and R denotes the shell radius; a is the base radius; $W(r,t)$ and $U(r,t)$ are displacement components along normal and tangential directions at time t, respectively, and $W_i(r,0)$ is the initial imperfection. The undeformed shape of the perfect shell can be adequately described by

$$z = H\left[1 - (r/a)^2\right] \tag{1}$$

where r is the radial coordinate.

The general differential equations for the response of spherical caps with initial imperfections are given in Ref. [4]. In this paper, we consider only the situation of the axisymmetric deformation with the inclusion of dynamic effects. The equilibrium equations associated with this situation are

$$D\nabla^4 W - N_r\left(W_f'' + \frac{1}{R}\right) - N_\theta\left(\frac{W_f'}{r} \quad \frac{1}{R}\right)$$

$$-q = -\rho h\ddot{W} \tag{2a}$$

$$(rN_r)' - N_\theta = r\rho h\ddot{U} \tag{2b}$$

where $\nabla^2(\ ) = (\ )'' + (\ )'/r$; $D = Eh^3/12(1 - \nu^2)$, E is Young's modulus, h is the shell thickness, ν is the Poisson's ratio, and ρ is the mass per unit volume of shell; prime and dot denote differentiations with respect to r and t, respectively, and θ is the circumferential coordinate; $q(r,t)$ is the applied loading and $W_f = W_i + W$; stress resultants are related to strains by

$$\begin{aligned} N_r &= \left[Eh/(1 - \nu^2)\right](\bar{\varepsilon}_r + \nu\bar{\varepsilon}_\theta) \\ N_\theta &= \left[Eh/(1 - \nu^2)\right](\bar{\varepsilon}_\theta + \nu\bar{\varepsilon}_r) \end{aligned} \tag{3}$$

in which strains are expressed in terms of displacements by

$$\begin{aligned} \bar{\varepsilon}_r &= U' - \frac{W}{R} + \frac{1}{2}(W')^2 + W'W_i' \\ \bar{\varepsilon}_\theta &= \frac{U}{r} - \frac{W}{R} \end{aligned} \tag{4}$$

The terms on the right hand sides of Eqs. (2) are the inertia forces due to normal and radial displacements of the shell. For convenience, the following nondimensional quantities and operations are introduced:

$$
\begin{aligned}
&x = r/a && m^4 = 12(1 - \nu^2) \\
&R = a^2/2H && q_{cr} = 4Eh/R^2m^2 \\
&\lambda^2 = m^2a^2/Rh && p(r,t) = q(r,t)/q_{cr} \\
&(\,)' = \partial(\,)/\partial x && (\dot{}) = \partial(\,)/\partial\tau \\
&\tau = \sqrt{E/\rho R^2}\,t && u = aU/h^2 \\
&w = W/h && w_i = W_i/h
\end{aligned}
\tag{5}
$$

where q_{cr} is the classical buckling pressure of a complete spherical shell of the same redius of curvature and thickness.

With the adoption of Eqs. (5), the nondimensional forms of Eqs. (2) become

$$
\begin{aligned}
&\nabla^4 w - 12(\varepsilon_\theta + \nu\varepsilon_r)\,(\nabla^2 w + \nabla^2 w_i) \\
&\quad - 12(1 + \nu)\,\frac{\lambda^2}{m^2}\,(\varepsilon_r + \varepsilon_\theta) \\
&\quad - 12(1 - \nu)\,(\varepsilon_r - \varepsilon_\theta)\,(w'' + w_i'') \\
&\quad - 4\,\frac{\lambda^2}{m^2}\,p = -\lambda^4 \ddot{w}
\end{aligned}
\tag{6a}
$$

$$
u'' + \frac{u'}{x} - \frac{u}{x^2} + g(w) = 0 \tag{6b}
$$

Where ε_r and ε_θ are nondimensional quantities of $\bar{\varepsilon}_r$ and $\bar{\varepsilon}_\theta$, respectively:

$$
\begin{aligned}
&\varepsilon_r = u' - \frac{\lambda^2}{m^2}\,w + \frac{1}{2}(w')^2 + w'w_i' \\
&\varepsilon_\theta = \frac{u}{x} - \frac{\lambda^2}{m^2}\,w
\end{aligned}
\tag{7}
$$

and

$$g(w) = f_r'(w) + \nu f_\theta'(w) + (1 - \nu)\left[f_r(w) - f_\theta(w)\right]/x$$

$$f_r(w) = -\frac{\lambda^2}{m^2} w + \frac{1}{2}(w')^2 + w'w_i'$$

$$f_\theta(w) = -\frac{\lambda^2}{m^2} w \tag{8}$$

$$f_r'(w) = -\frac{\lambda^2}{m^2} w' + w'w'' + w'w_i'' + w''w_i'$$

$$f_\theta'(w) = -\frac{\lambda^2}{m^2} w'$$

It is noted that, in view of the assumed shallowness, the effect of radial inertia force is neglected in Eq. (6b). Eqs. (6) constitute the basic equations for the analysis subjected to prescribed boundary conditions. Boundary condition considered in this paper are clamped:

$u(1,\tau) = w(1,\tau) = w'(1,\tau) = 0$. Due to symmetry at the apex, we also have $u(0,\tau) = w'(0,\tau) = 0$.

METHOD OF SOLUTION

Eqs. (6) are not only lengthy but also highly nonlinear in w, the major variable. The solution plan is to superpose a finite-difference mesh on the one-dimensional shell domain, replace nonlinear differential equations Eqs. (6) by a set of two nonlinear algebraic finite-difference equations, and solve the resulting set of equations by the nonlinear relaxation method.

Details of the nonlinear relaxation technique will not be discussed here; description of the technique is given in references [16,17]. Simply put, the nonlinear relaxation technique offers a method of systematically reducing the errors at each nodal point for each algebraic equation to some acceptable level.

Rather than solving all two differential equations simultaneously, we elect to solve first the w system of difference equations in an iterative manner, and subsequently the u system of equations. We revert back to the w system again and the u and so on, until the percentage change of the displacement at all nodal points is always less than 0.0001 percent on the (absolute) average.

The second time derivative of w in Eq. (6a) is approximated by the Houbolt's third-order buckwards difference expression [18]:

$$\ddot{w}(x,\tau) = (1/\delta^2)\left[2w(x,\tau) - 5w(x,\tau - \delta) + 4w(x,\tau - 2\delta) - w(x,\tau - 3\delta)\right] \tag{9}$$

where $\delta = \Delta\tau$ is the equal time increment.

The accuracy of this representation is of order δ^2. Special attention is devoted to the first few time steps where Eq.(9) cannot be applied directly. Before giving the expression for these first few time steps, we note that the initial conditions are of the form

$$w(x,0) = 0 \qquad \dot{w}(x,0) = 0 \tag{10}$$

From Eq.(10), expression of Eq. (9) for the first few time steps can readily be obtained as (Ref. [10])

1) $\tau = 0$, $w(x,0) = 0$

2) $\tau = \delta$; since $\dot{w}(x,0) = 0$, we have $w(x,-\delta) = w(x,\delta)$ and hence $\ddot{w}(x,\delta) = (2/\delta^2)\, w(x,\delta)$

3) $\tau = 2\delta$; $\ddot{w}(x,2\delta) = (2/\delta^2)\left[w(x,2\delta) - 3w(x,\delta)\right]$

4) $\tau > 2\delta$, Eq.(9) can be applied directly.

In our numerical computation, the number of nodal points are selected such that a subsequent increase in nodal points does not significantly affect the magnitude of the static buckling load. With this consideration, 14 nodal points for $\lambda = 5$ and up to 22 points for $\lambda = 10$ are adopted; A Poisson's ratio of 1/3 is also used. A time step must be selected very judiciously. A good selection is such that the results are within a desired accuracy, but not too small in light of computer time considerations. A reasonable compromise of equal time increments of $\delta = 0.10$ is used; this same time increment is also selected in Ref. [11].

DYNAMIC BUCKLING CRITERION

Criteria for dynamic axisymmetric buckling of the shallow spherical shell are not as well defined as for static buckling, and require an evaluation of the transient response of the shell for various load levels.

The criterion adopted most widely (Refs. [10,11,12,14]) is based on plots of the peak nondimensional average displacement in time history, Δ max, of the shell structure versus the amplitude of the load where Δ is the average displacement and has been defined [11,14] in dimensionless form as follows:

$$\Delta = \int_0^a rW dr \; / \int_0^a rz dr \qquad (11)$$

The numerator is the volume generated by the shell deformation and the denominator is the constant volume under the cap.

There is a load range where a sharp jump in peak average displacement occurs for a small change in load amplitude. The inflection point of the load deflection curve in this range is regarded as the buckling load; this procedure is called the "inflection point method". When the buckling load is defined in this manner, it is also referred to as the dynamic snap-through load.

The method is demonstrated by a typical example shown in Fig. 2 . In this figure, $\Delta - \tau$ curves are displayed for several uniform load parameters p (this example is related to a clamped spherical cap of $\lambda = 5$ under step uniform pressure of infinite duration). A plot of Δ_{max} vs. p based on information given in Fig. 2 is shown in Fig. 3 . It is clear from this figure that there is a sharp jump at p = 0.46, and according to the criterion defined above, this value is taken as buckling pressure for this particular spherical cap geometry and load situation.

CHECKS WITH EXISTING SOLUTIONS FOR PERFECT CAPS

The general program developed for buckling of spherical caps with initial imperfections [3,4] is modified to account for the simpler axisymmetric spherical cap under dynamic loading. In order to test the validity of this modified program, computer runs are made to determine dynamic buckling loads of spherical caps for which numerical results exist.

Fig. 2 represents $\Delta - \tau$ curves for different load levels for the axisymmetric spherical cap of $\lambda = 5$ under uniform step pressure of infinite duration; the $\Delta_{max} - p$ curve associated with Fig. 2 is given in Fig. 3 . According to the dynamic buckling criterion described earlier, dynamic buckling loads for $\lambda = 5$ under step loading is taken as $p_{cr} = 0.46$ (where p_{cr} is denoted as the dynamic buckling or snap-through load).

Computer runs also are made for $\lambda = 7.5$ and 10; the $\Delta - \tau$ curves of these two geometric parameters are shown in Figs. 4 and 5 , respectively. A summary of these values along with the results obtained elsewhere are tabulated in Table 1 for comparison. It is found from this Table that the present values are in very good agreement with solutions presented in Refs. [10-12,14].

Table 1 Dynamic Buckling Pressure for Various Values of Spherical Cap Parameters

λ	5	7.5	10
Present	.46	.44	.49
Ref. 10	.49	.5	.42
Ref. 11	.45	.44	.37
Ref. 12	.48	.51	.50
Ref. 14	.48	.5	.43

The present solution is carried out using time steps $\delta = 0.10$ with 14 to 22 meridional finite difference stations for $\lambda = 5$ to 10. The length of response calculation time τ carried out in computer runs is varied from case to case with the criterion that, in the neighborhood of the buckling load, τ is sufficiently large enough to allow $\Delta - \tau$ curves to fully develop. As a result we obtain more accurate buckling loads, and save computer time when load levels are other than in the neighborhood of the buckling pressure. More discussion in this regard will be provided in the next section.

It is interesting to note from Table 1 that the magnitude of dynamic buckling loads is not sensitive to shell geometry λ. This finding suggests that the dynamic buckling load obtained for spherical caps represents the value for the complete spherical shell. However, this observation does not apply to the static buckling situation, since results obtained in this study show that static buckling loads are 0.65, 1.02 and 0.85 for $\lambda = 5$, 7.5 and 10, respectively.

DYNAMIC BUCKLING OF SPHERICAL CAPS WITH INITIAL IMPERFECTIONS

With the validity of the computer program established for dynamic buckling analysis as demonstrated in the previous section, we now proceed to investigate the effect of initial imperfections on the dynamic buckling capacity of spherical caps. We shall also examine how different types of loadings with various time duration affect the dynamic buckling loads.

Two types of dynamic loadings are considered herein, namely, uniform step pressure of infinite duration and a right triangular pulse with various time duration. Solutions obtained in this study will give some indications on the most severe type of dynamic loading situations. Specific results on these two types of loading situations are discussed separately in this section.

The axisymmetric initial imperfection adopted in this study is of the dimple type which was also used by Koga and Hoff [2]. This type of imperfection is expressed mathematically as

$$w_i = (W_o/h)\,(1 - x^2)^3 \qquad (12)$$

where W_o is the maximum imperfection which occurs at the shell apex. Selection of this expression is, in fact, quite arbitrary; however, it does provide an adequate description for actual shells since the important parameter is the maximum eccentricity and not the imperfection shape function.

Since dynamic buckling pressure is not sensitive to spherical cap geometric parameter (λ) as can be seen from Table 1, we select $\lambda = 5$ for all analyses in this section.

Step Loading

Let us first consider buckling analysis of the axisymmetric spherical cap ($\lambda = 5$) with initial imperfections under a uniform step loading of infinite duration. Some typical Δ - p curves associated with various load levels are given in Fig. 2 . From this figure, it is noted that a different response calcualtion time τ has been utilized for different load levels. Although the reason for using this strategy was mentioned briefly in the last section, a more detailed discussion in this regard is given here. As is apparent from Fig. 2 the peak value of Δ occurs after several cycles of oscillation for the load level p above the critical value of p for snap-through (we shall call this value p_{cr} the dynamic buckling or dynamic snap-through load). It is also observed that for the load levels above p_{cr}, the larger the value of p, the smaller the response calculation time taken for Δ to reach its peak value. Clearly, a flexible response calculation time is desired to cope with various load situations.

The strategy initiated here stems from the fact that in dynamic analysis with significant nonlinearity, time consuming iteration schemes and a huge number of time steps are usually involved. This strategy perhaps can best be accomplished through the execution of the computer program in an interactive mode. By inserting some simple statements in the program, execution of the program will pause after a fixed period of response calculation time and the user can decide to continue or terminate the execution depending on whether Δ has reached its peak value. On the other hand, for a load range very close to p_{cr} , sufficient response calcualtion time should be given to insure that the shell structure does not eventually buckle.

This approach should predict more accurate buckling loads and will also save considerable computing time. Huang [10] carried his solution for $\lambda = 5$ out to $\tau = 14$ using a very fine time increment $\delta = 0.02$ and $(4\lambda + 1)$ stations.

Stephens and Fulton [11] obtained their solution up to $\tau = 60$ for $\lambda = 5$ and $\tau = 120$ for higher values of λ by using $\delta = 0.10$ and 20 stations. Ball and Burt [14] carried their results out to $\tau = 50$ for $\lambda = 5$, and $\tau = 120$ for $\lambda = 8$ and 11 stations with $\delta = 0.05$. As mentioned earlier, in the present calculations, we employ different response calculation times for different load situations; $\delta = 0.10$ and 14 to 22 stations for $\lambda = 5$ to 10 are selected. The convergence criterion adopted is that the average absolute percentage change of displacement functions is less than 0.0001.

With adoption of this strategy for the selection of response calculation time, a series of runs are made for an axisymmetric spherical cap ($\lambda = 5$) with different magnitudes of initial imperfections. Fig. 6 represents the Δ_{max} - p curves for this shell geometry with imperfections W_o/h ranging from 0.1 to 1.0. Aslo included in this figure for comparison purposes is the result for the perfect shell which has already been displayed in Fig. 3 . According to the dynamic buckling criterion described earlier in this paper, the dynamic buckling loads (p_{cr}) are found to be 0.46, 0.39, 0.28 and 0.185 for imperfections of W_o/h = 0, 0.1, 0.5 and 1.0, respectively.

Sudden jump in Δ_{max} near the critical load area is very obvious for W_o/h = 0, 0.1 and 0.5. For the case of $W_o/h = 1.0$, the Δ_{max} -p curve does not exhibit such a drastic change in displacement and the inflection point technique is used to determine the magnitude of the buckling load. Suffice it to say that the sudden jump phenomenon may be viewed as a particular case of the situation whose dynamic buckling load must be determined by the inflection point method. Therefore, the inflection point method can be regarded as a more general means to obtain dynamic buckling loads.

A plot of p_{cr} vs. W_o/h based on the results displayed in Fig. 6 is shown in Fig. 7 . From this figure it is obvious that initial imperfections do indeed have the effect of reducing dynamic buckling capacity of spherical caps.

For comparison purposes, static buckling loads are also obtained for the same shell geometry and initial imperfections, and these results are also superposed in Fig. 7 . It is noted from this figure that the two curves intersect at about $W_o/h = 0.74$. It is observed from this figure that, when comparing with dynamic buckling loads, static response yields higher buckling values for W_o/h in between 0 and 0.74, but, on the other hand, has a lower buckling value when W_o/h is greater than 0.74. Evidentally, when imperfections exist, the static response reduces shell buckling capacity at a faster rate than that by dynamic response. In other words, static response of axisymmetric spherical caps is more sensitive to initial imperfections than dynamic response. This finding is significant in shell structure design if initial imperfections are taken into consideration.

Triangular Pulse

Having analyzed the dynamic buckling response of the spherical cap with an axisymmetric imperfection and a spatially and temporally constant pressure field, we turn next to the same problem except for the pressure pulse which is now taken as triangular rather than constant with time. The right triangualr pulse shown in the subset of Fig. 8 is taken as representative of this type of loading. At dimensionless time τ^* the pressure has a zero value.

Except for some minor modifications made to deal with the time-varying nature of applied loading, the same computer program and strategy described earlier are utilized for this analysis.

Four triangle pulses with duration $\tau^* = 0.544$, 2.176, 10.88 and 21.76 are considered. The same spherical cap geometry ($\lambda = 5$) and magnitude of imperfections are retained. Fig. 8 presents the results of the axisymmetrical spherical cap under triangle pulse of $\tau^* = 0.544$ and with imperfections $W_o/h = 0$, 0.1, 0.5 and 1. According to the dynamic buckling criterion adopted in this paper, buckling loads are discerned as 5.05, 4.8, 3.95, and 3.1 for $W_o/h = 0$, 0.1, 0.5, and 1, respectively. Figs. 9 , 10 , and 11 display the results associated with triangular pulse durations $\tau^* = 2.176$, 10.88 and 21.76, respectively.

A summary of numerical results shown in these figures is given in Table 2 for comparison. Also included in this table are the values for static response and step loading of infinite duration. In addition to buckling loads, Table 2 also gives for most situations the dimensionless buckling time and finite difference node where plasticity begins. One interesting and important observation made from this table is that, for the cases of very short triangular pulses ($\tau^* = 0.544$ and 2.176), the spherical cap buckles after removal of the pulses. Evidently, the kinetic energy imparted to the cap by the pressure pulse was enough to propel the cap into a buckling mode

Table 2 Dynamic and Static Buckling Loads for A Clamped Axisymmetric Spherical Cap ($\lambda = 5$)**

Loading	Imperfection, W_o/h											
	0			0.1			0.5			1.0		
	B	T	L	B	T	L	B	T	L	B	T	L
Static	0.65		—	0.55		—	0.33		—	0.14		—
Dynamic												
Step Loading	0.46	23	—	0.39	30.5	14	0.28	21.5	14	0.185	15	3
Triangular Pulse												
$\tau^* = 0.544$	5.05	2.6	—	4.8	7.8	4	3.95	1.7	3	3.1	4.0	7
2.176	1.55	3.5	7	1.45	4.3	8	1.15	3.5	7	0.775	4.3	7
10.88	0.685	7.75	12	0.615	7.8	6	0.4	7.0	3	0.26	7.4	3
21.76	0.565	12.4	13	0.51	8.7	3	0.335	8.5	5	0.215	6.5	3

** B, T, L and τ^* in this Table, respectively, stand for

B = Buckling load

T = Dimensionless buckling time (some of these values are obtained by interpolation)

L = Finite difference node where plasticity begins (See Fig. 12) (some of these values which were not calculated in earlier computer runs are shown with -)

τ^* = Dimensionless time duration of triangular pulse (at $\tau = \tau^*$, traingular pulse has a zero value, see subset of Fig. 8)

well after load removal. An examination of L nodes provided in this table reveals that no regular pattern is developed for the location as to where plasticity may begin (Mises criterion utilized).

Fig. 13 exhibits the relationship between dynamic buckling load p_{cr} and pulse duration τ^* for different magnitudes of imperfections. This figure demonstrates that the length of τ^* has a very significant effect on the magnitude of the dynamic buckling load. For the same W_o/h, this figure shows that dynamic buckling load for $\tau^* = 0.544$ is about 9 to 11 times greater than that for $\tau^* = 21.76$.

Fig. 14 gives the curves for dynamic buckling load versus initial imperfection for various triangular pulse durations. Also shown for comparison purposes is the result of step loading which was displayed in Fig. 7. As can be seen from this figure that, for a given magnitude of imperfection, the shorter the triangular pulse, the higher the buckling load. This figure also reveals that the limiting case of triangular pulse of various time durations is the step loading of infinite duration. It is important to point out that this limiting case represents the most severe loading situation for dynamic buckling analysis, since it yields the lowest values of dynamic buckling loads.

DISCUSSION AND CONCLUSIONS

An investigation has been carried out for dynamic buckling analysis of axisymmetrical spherical caps with initial imperfections. Two types of loading are considered, namely, step pressure of infinite duration and triangular pulses of various time durations. Governing equations given in Refs. [3,4] for buckling analysis of spherical caps with asymmetric imperfections are modified to account for the axisymmetric nature of the problem and dynamic effects. Central finite differences and Houbolt's backwards difference scheme [18] are used to replace spatial and temporal derivatives, respectively. The nonlinear relaxation method [16,17] is then employed to solve the resulting algebraic equations.

Unlike static buckling analyses, dynamic buckling loads are determined from a displaced volume-pressure (Δ_{max} - p) curve by the inflection point method [11]. Dynamic snap-through occurs when there is a sharp jump in the Δ_{max} - p curve [10]. This indicates that the maximum amplitude of oscillation of the shell has a discontinnous change.

To verify possible validity of the present computer program, a series of runs are made to determine dynamic buckling loads for axisymmetrical spherical caps of λ = 5, 7.5, and 10 under uniform step loading of infinite time duration. Current results along with previous findings [10-14] are tabulated in Table 1 for comparison. Good agreement among these solutions is observed; it may be concluded that the inflection point method has been generally accepted as a dynamic buckling criterion.

Since dynamic buckling loads are not sensitive to shell geometry as can be seen from Table 1, we select λ = 5 for all analyses in this paper. A dimple type of imperfection is also adopted in this study which provides a very adequate description of the local nature of initial imperfections in spherical shells.

Results of the axisymmetric spherical cap ($\lambda = 5$) under step loading are obtained for maximum imperfections of $W_o/h = 0.1$, 0.5 and 1.0. These results are displayed in Fig. 6 along with that of the perfect shell. Buckling loads obtained from Fig. 6 by the inflection point method are presented in Fig. 7 . Also displayed in Fig. 7 , for comparison purposes are the solutions from static buckling analysis. It is observed from this figure that, for W_o/h less than about 0.74, the static buckling load is higher than the dynamic buckling load. However, when W_o/h is greater than 0.74, the above situation is reversed. This result demonstrates that the static buckling load decreases more rapidly than the dynamic buckling load because of imperfections. Moreover, the static response is more sensitive to initial imperfections than the dynamic response.

It is important to point out that imperfections do indeed have the effect of reducing buckling capacity for both static and dynamic responses, although they are affected in different manners.

Calculations are also carried out for the same shell geometry with the same magnitude of imperfections under right triangular pulses. Four different pulse durations are considered, namely, $\tau^* = 0.544$, 2.176, 10.88 and 21.76. Results of Δ_{max} - p for these four cases are shown in Figs. 8-11 , respectively. Dynamic buckling loads obtained from these figures are displayed against pulse duration τ^* in Fig. 13 for various magnitudes of imperfection and against initial imperfection in Fig. 14 for different pulse durations. Also displayed in Fig. 14 is the solution for the step loading. From Fig. 13 , it is found that pulse duration has a very significant impact on the magnitude of dynamic buckling load. For example, for the same imperfection, dynamic buckling load for $\tau^* = 0.544$ is about 10 times higher than that for $\tau^* = 21.76$. This observation can also be seen from Fig. 14 . In fact, Fig. 14 shows that the limiting case of the triangular pulse is the step loading of infinite duration, and that

the step loading represents the most severe loading situation for dynamic buckling analysis, since it yields the lowest values of buckling loads.

A summary of results displayed in Fig. 8-11 along with those of static and dynamic step loadings of infinite duration is given in Table 2 for comparison purposes. In addition to buckling loads, Table 2 also provides information for the buckling time and finite difference node where plasticity begins. Two observations are made: first, for the cases of very short triangular pulses ($\tau^* = 0.544$ and 2.176), the spherical cap buckles after removal of the pulses; secondly, no regular pattern is developed for the location as to where plasticity may begin.

As a final remark, the flexible response calculation time option set up in the computer program enables users to continue or terminate the execution. This option not only provides a possibility of obtaining more accurate dynamic buckling loads, but also saves considerable computing time for the cases where additional execution appears to be unnecessary.

REFERENCES

(1) Hutchinson, J.W., "Imperfection sensitivity of externally pressurized spherical shells," Journal of Applied Mechanics, Vol. 34, no. 1, Trans. ASME, Vol.89 , Series E, March 1967, pp. 49-55.

(2) Koga, T., and Hoff, N.J., "The axisymmetric buckling of initial imperfection complete spherical shells," SUDDAR 332, May 1968, Stanford University.

(3) Kao, R., and Perrone, N., "Asymmetric buckling of spherical caps with asymmetric imperfections," Journal of Applied Mechanics, Vol. 38, series E, no. 1, March 1971.

(4) Kao, R., "A note on buckling of spherical caps with initial asymmetric imperfections," Journal of Applied Mechanics, Vol. 39, series E, no. 3, Sept. 1972.

(5) Humphrey, J.S., and Bodner, S.R., "Dynamic buckling of shallow shells under impulsive loading," Journal of Engineering Mechanics Division, Proceedings of Americal Society of Civil Engineers, Vol.88, EM2, April 1962, pp. 17-36.

(6) Budiansky, B. and Roth, R.S., "Axisymmetric dynamic buckling of clamped shallow spherical shells," TND-1510, 1962, NASA, pp. 597-606.

(7) Simitses, G.J., "Axisymmetric dynamic snap-through buckling of shallow spherical shells," AIAA Journal, Vol. 5, no. 5, May 1967, pp. 1019-1021.

(8) Archer, R.R. and Lange, C.G., "Nonlinear dynamic behavior of shallow spherical shells," AIAA Journal, Vol. 3, no. 12, Dec. 1965, pp. 2313-2317.

(9) Lock, M.H., Okubo, S. and Whittier, J.S., "Experiments on the snapping of a shallow dome under a step pressure load," AIAA Journal, Vol. 6, no. 7, July 1968, pp. 1320-1326.

(10) Huang, N.C., "Axisymmetric dynamic snap-through of elastic clamped shallow-spherical shells," AIAA Journal, Vol. 7, no. 2, Feb. 1969, pp. 215-220.

(11) Stephens, W.B. and Fulton, R.E., "Axisymmetric static and dynamic buckling of spherical caps due to centrally distributed pressure," AIAA Journal, Vol. 7, no. 11, Nov. 1969, pp. 2120-2126.

(12) Stricklin, J.A. and Matinez, J.E., "Dynamic buckling of clamped spherical caps under step pressure loadings," AIAA Journal, Vol. 7, no. 6, June 1969, pp. 1212-1213.

(13) Stricklin, J.A., et al., "Nonlinear dynamic analysis of shells of revolution by matrix displacement method," AIAA Journal, Vol. 9, no. 4, April 1971, pp. 629-636.

REF. (cont.)

(14) Ball, R.E. and Burt, J.A., "Dynamic buckling of shallow spherical shells," Journal of Applied Mechanics, June 1973, pp. 411-416.

(15) Akkas, N., "Bifurcation and snap-through phenomena in asymmetric dynamic analysis of shallow spherical shells," Computers and Structures, Vol. 6, 1976, pp. 241-251.

(16) Perrone, N. and Kao, R., "Large deflection response and buckling of partially and fully loaded spherical caps," AIAA Journal, Vol. 8, no. 2, Dec. 1970.

(17) Perrone, N. and Kao, R., "A general nonlinear relaxation technique for solving nonlinear problems in mechanics," Journal of Applied Mechanics, Vol. 38, no. 2, June 1971, pp. 371-376.

(18) Houbolt, J.C., "A recurrence matrix solution for the dynamic response of elastic aircraft," Jounal of Aeronautical Science, Vol. 17, Sept. 1950, pp. 540-550.

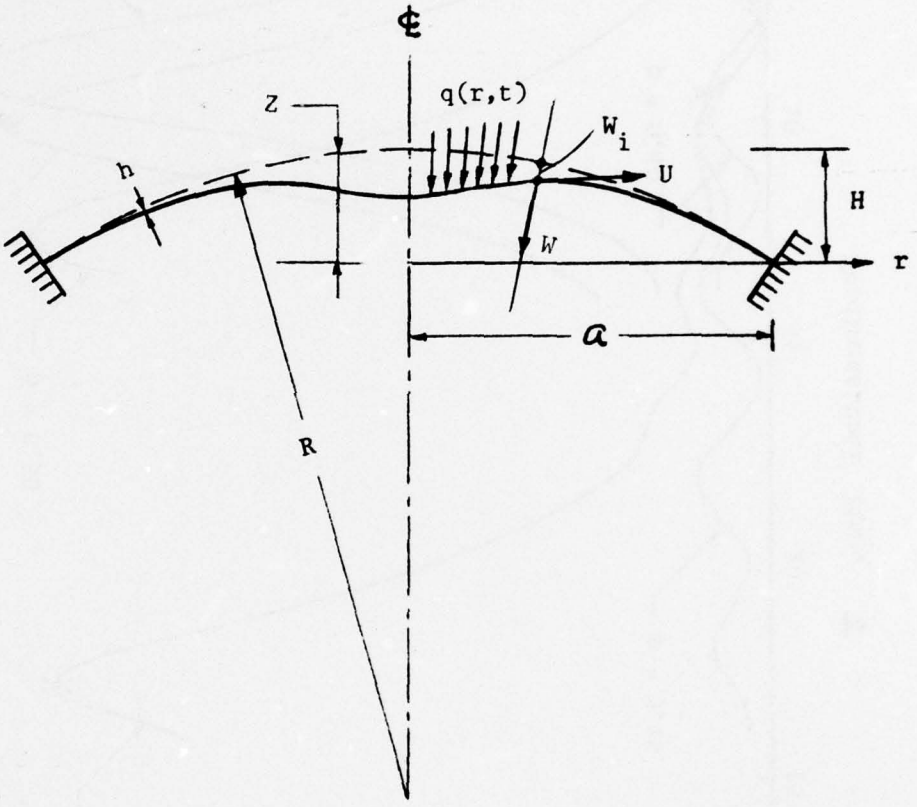

Fig. 1 Geometry of clamped spherical cap with axisymmetric imperfection.

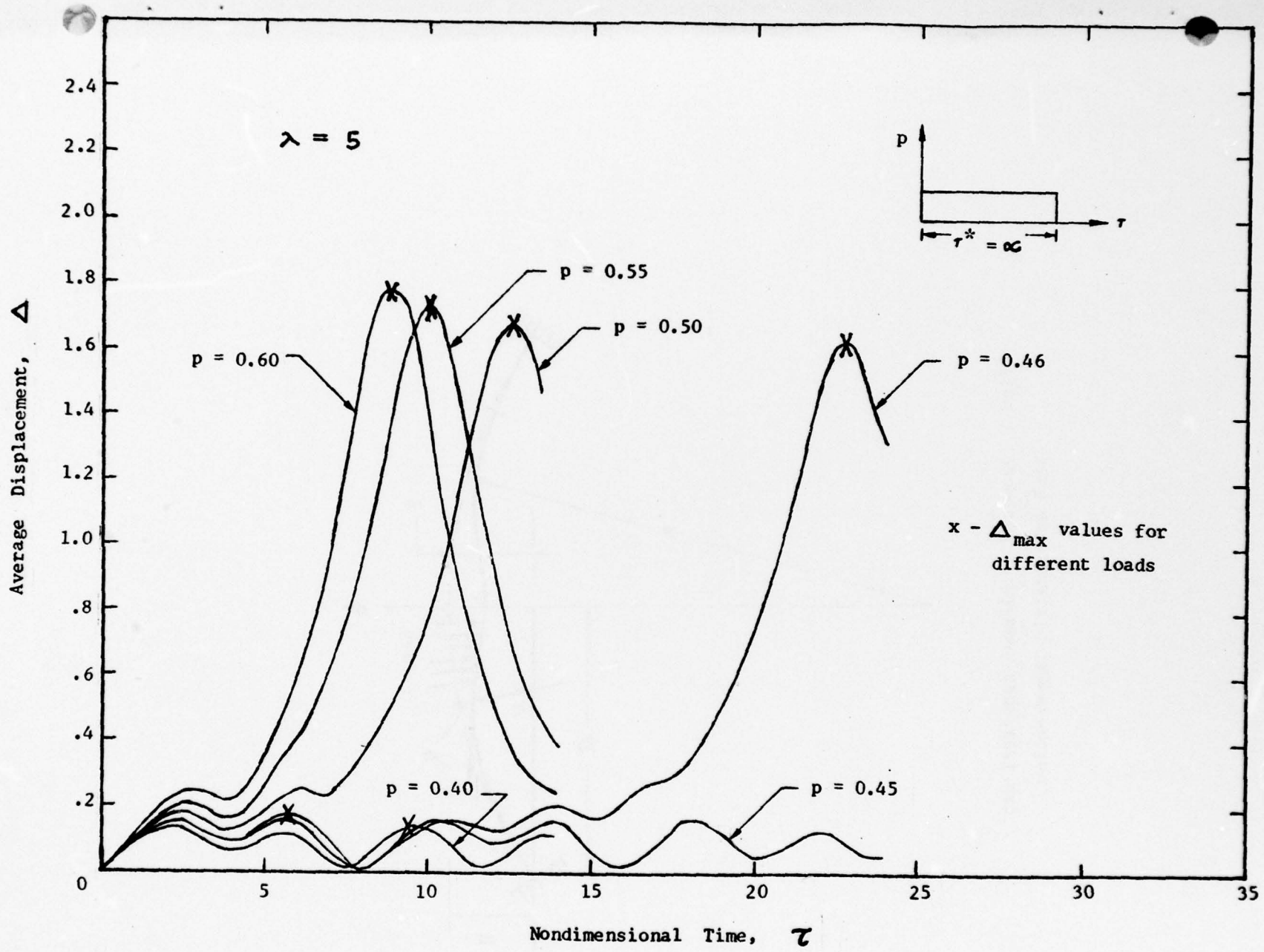

Fig. 2 Dynamic response of a clamped spherical cap (λ = 5) under uniform step loading of infinite duration.

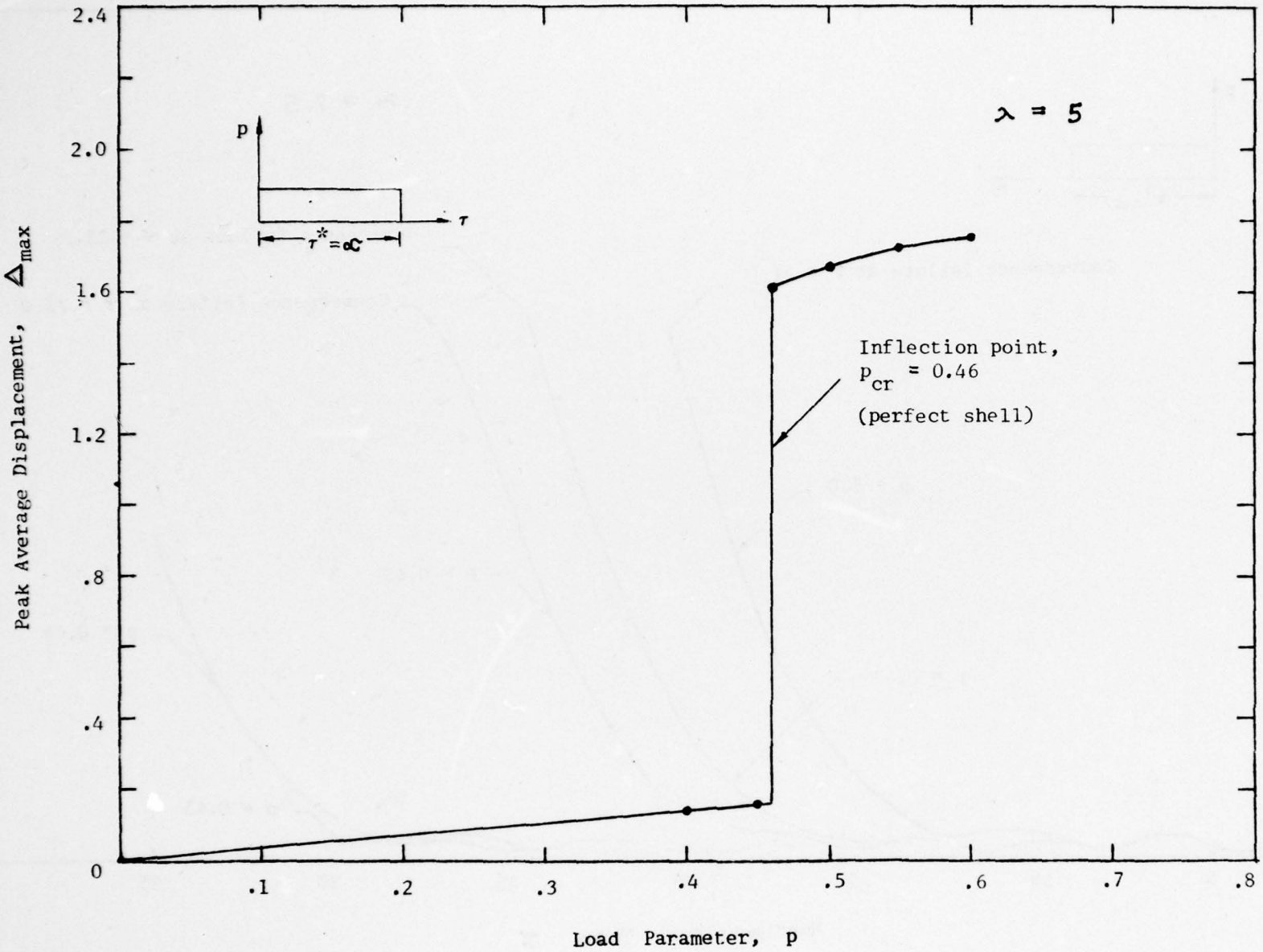

Fig. 3 Dynamic buckling load for a clamped spherical cap ($\lambda = 5$) under uniform step loading of infinite duration.

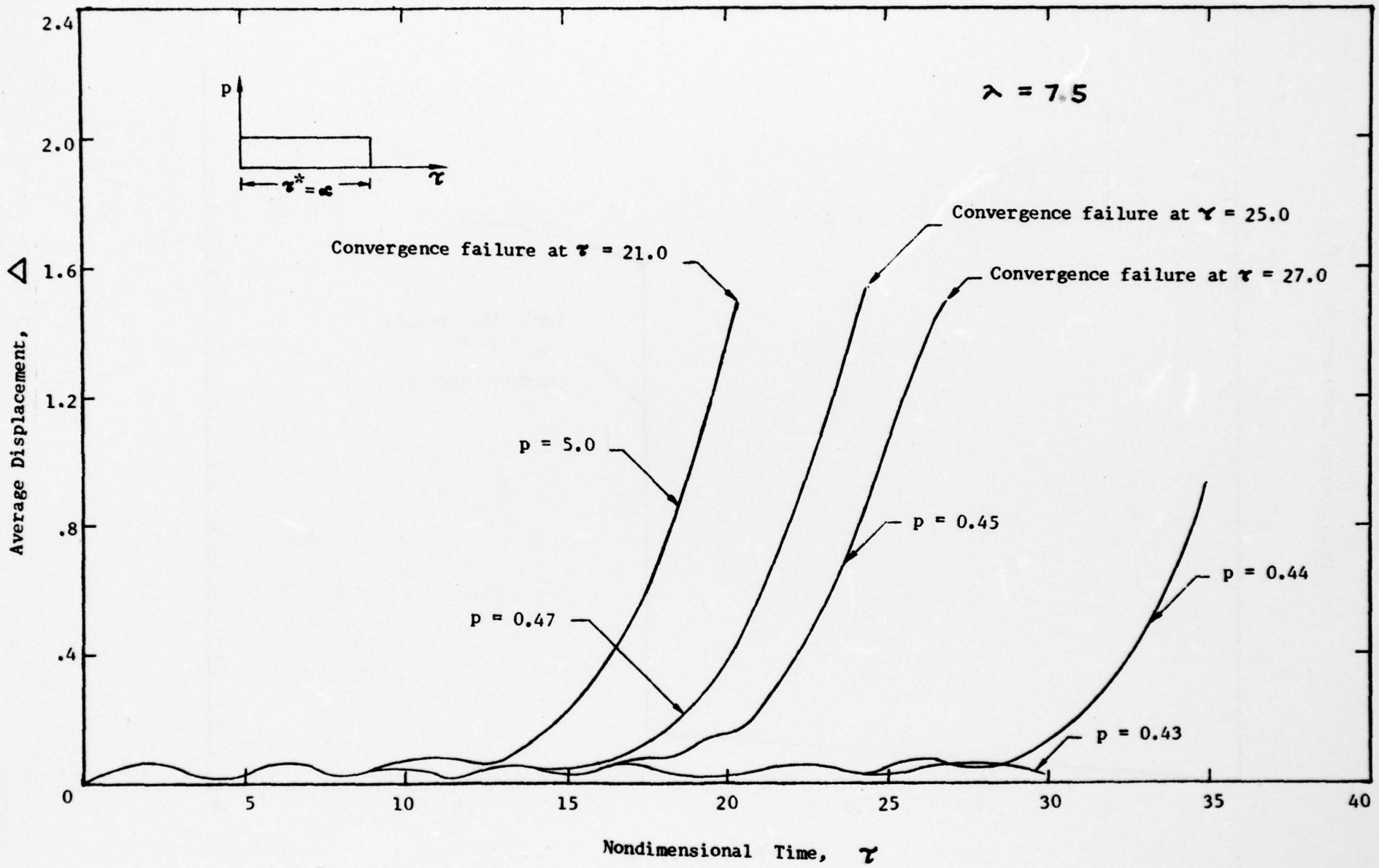

Fig. 4 Dynamic response for a clamped spherical cap (λ = 7.5) under uniform step loading of infinite duration.

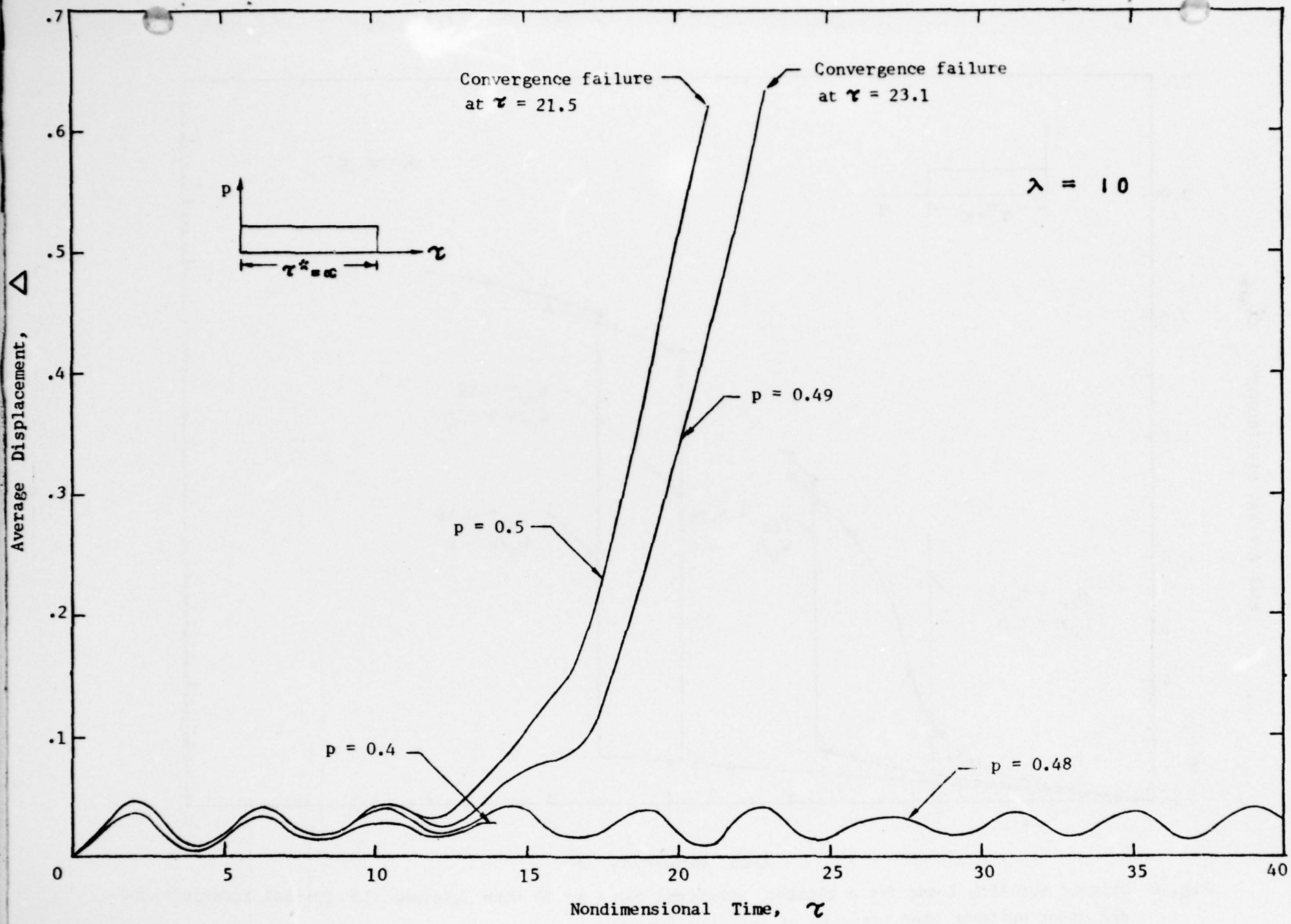

Fig. 5 Dynamic response for a clamped spherical cap ($\lambda = 10$) under uniform step loading of infinite duration.

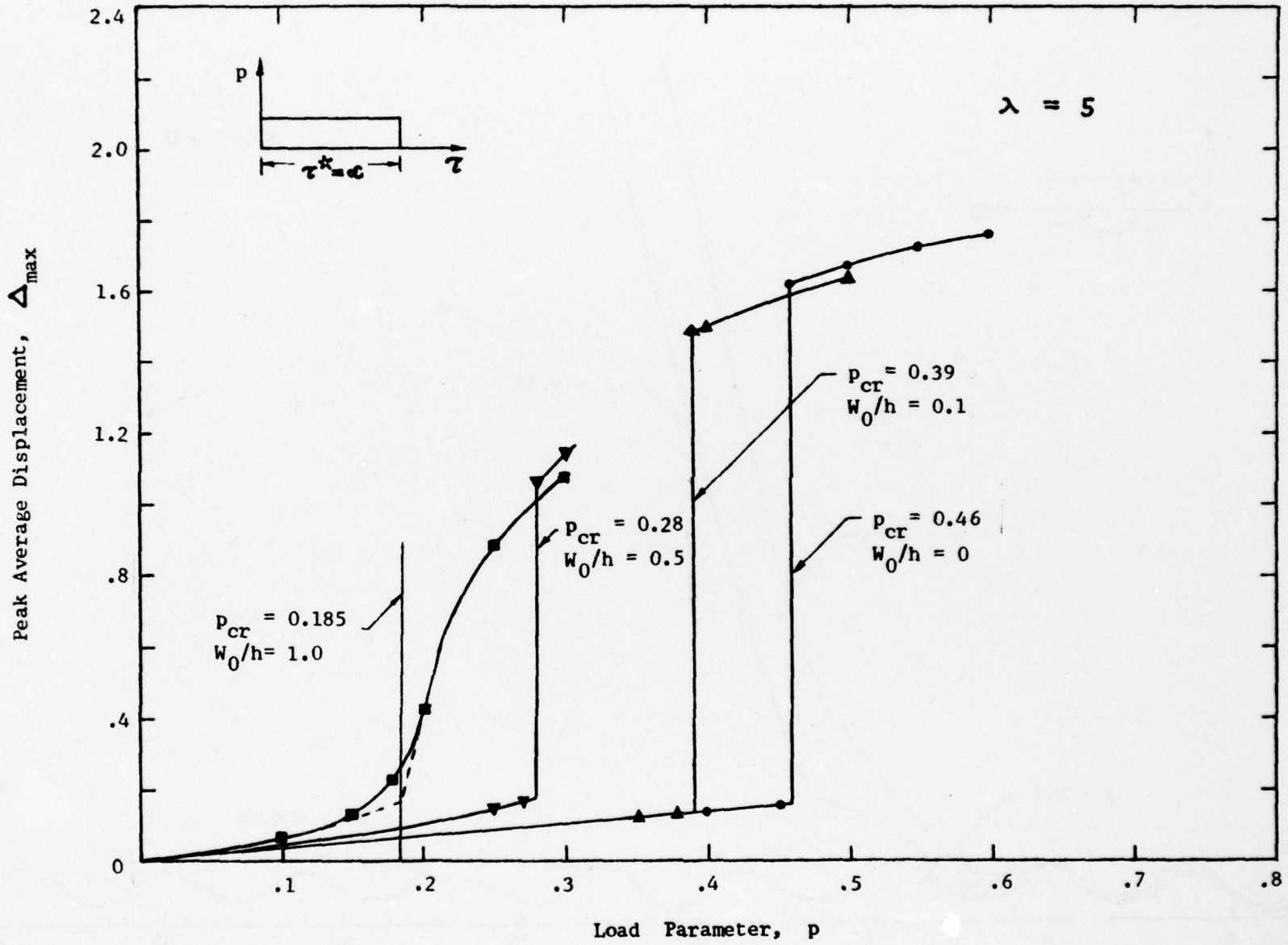

Fig. 6 Dynamic buckling loads for a clamped spherical cap ($\lambda = 5$) with axisymmetric initial imperfections and under uniform step pressure of infinite duration.

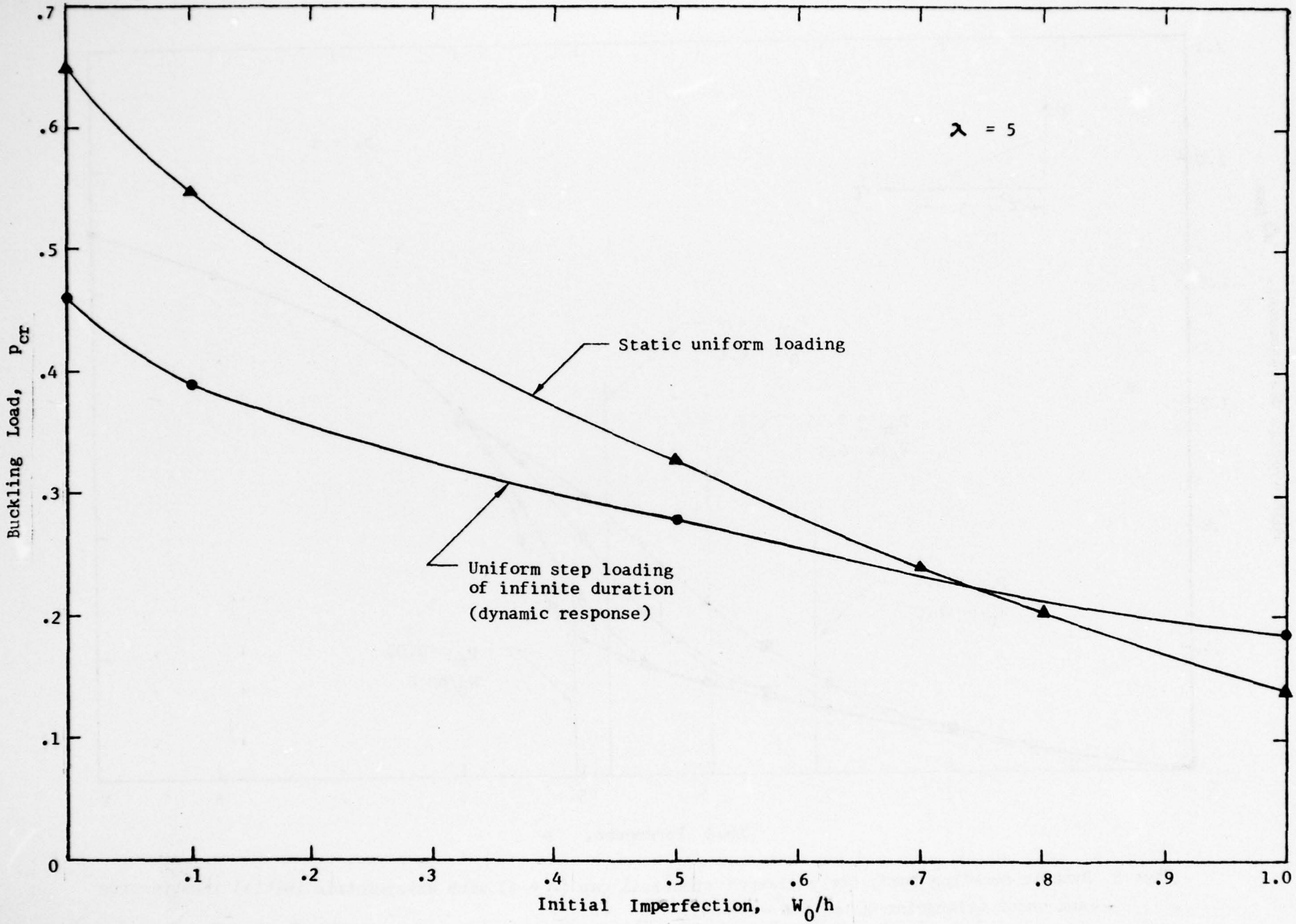

Fig. 7 Buckling load vs initial imperfection for an axisymmetric spherical cap ($\lambda = 5$).

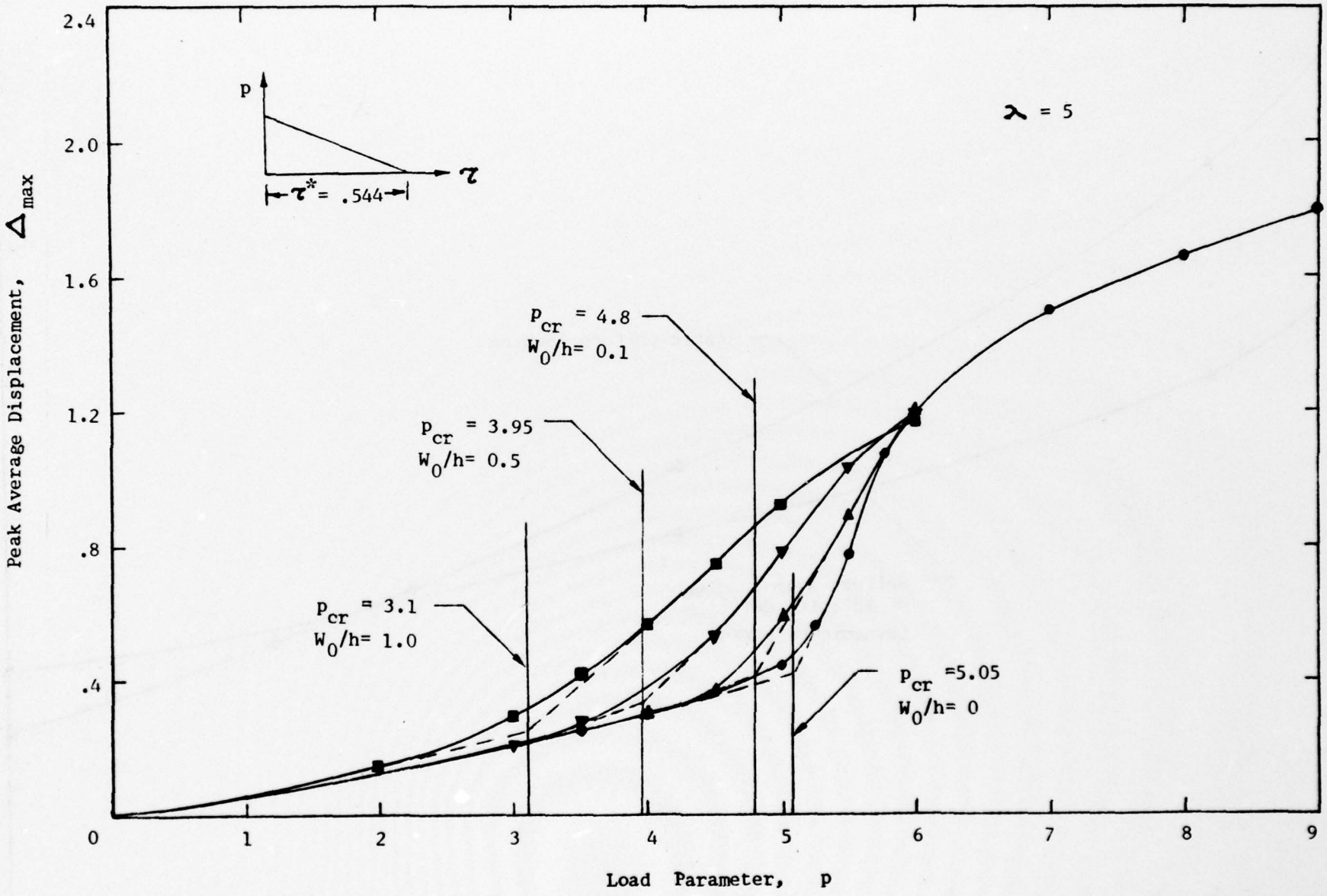

Fig. 8 Dynamic buckling loads for a clamped spherical cap (λ = 5) with axisymmetric initial imperfection and under triangular pulse (τ^* = .544).

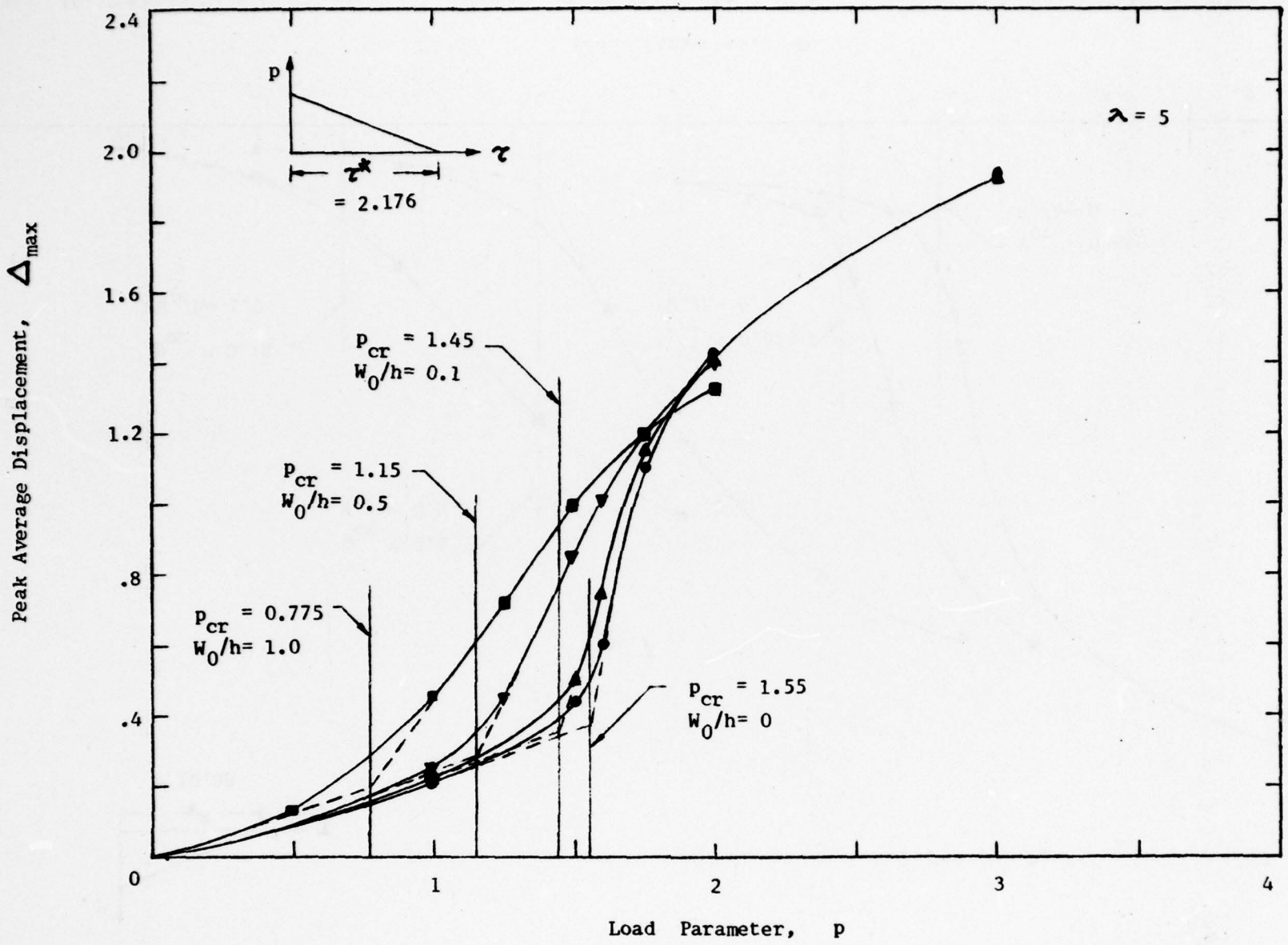

Fig. 9 Dynamic buckling loads for a clamped spherical cap (λ= 5) with axisymmetric initial imperfection and under triangular pulse (τ^*= 2.176).

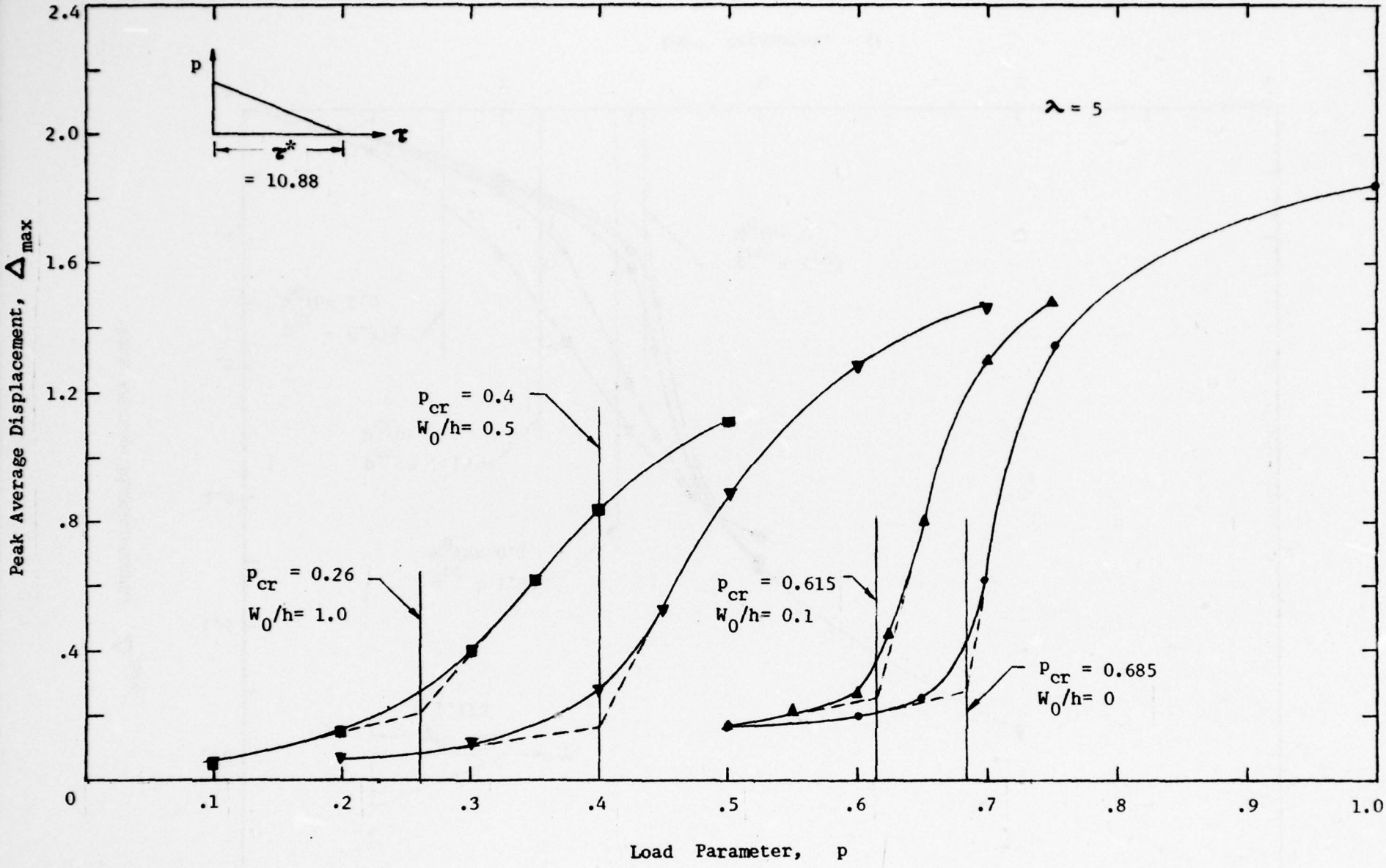

Fig. 10 Dynamic buckling loads for a clamped spherical cap ($\lambda = 5$) with axisymmetric initial imperfection and under triangular pulse ($\tau^* = 10.88$).

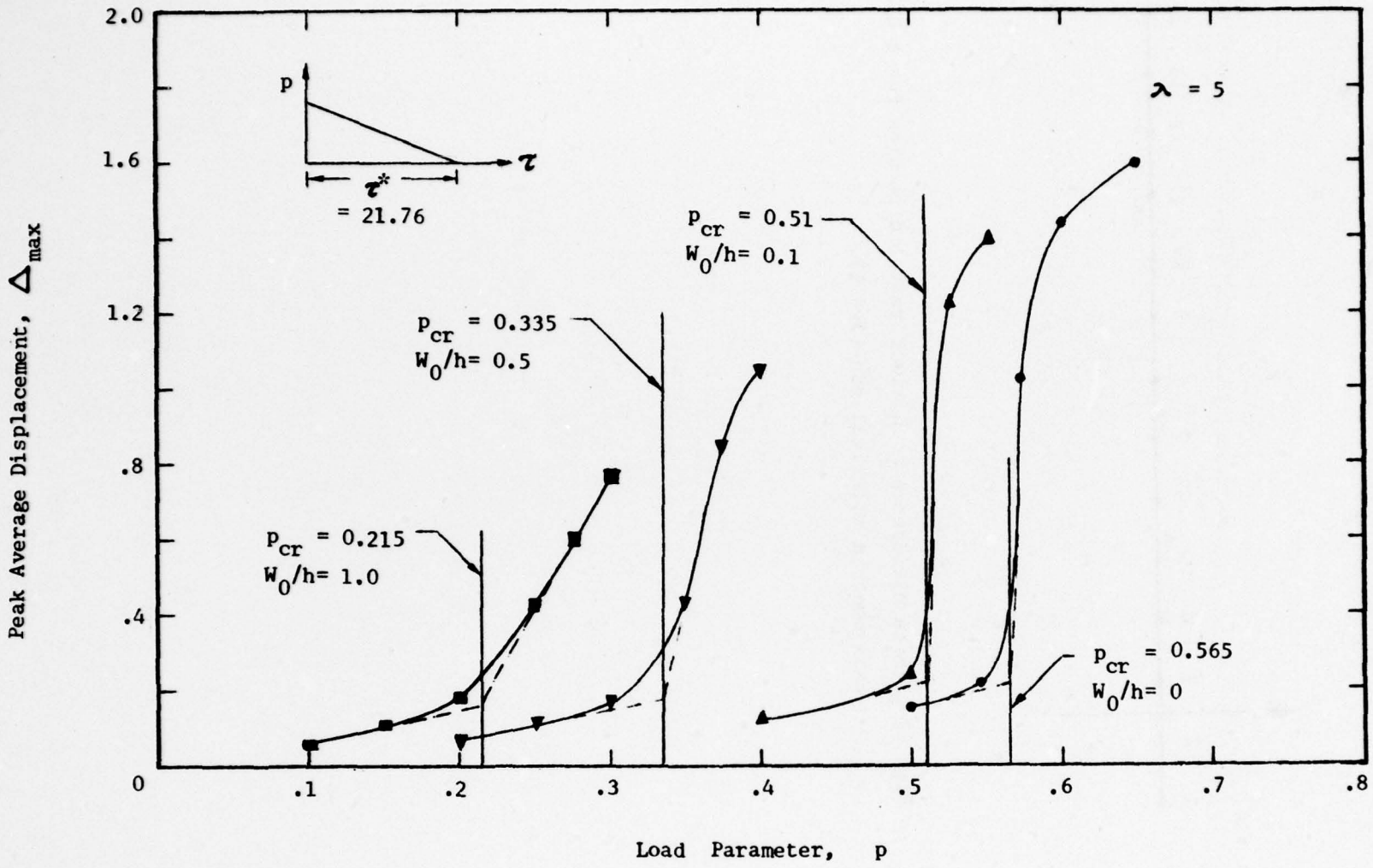

Fig. 11 Dynamic buckling loads for a clamped spherical cap (λ = 5) with axisymmetric initial imperfection and under triangular pulse (τ^* = 21.76).

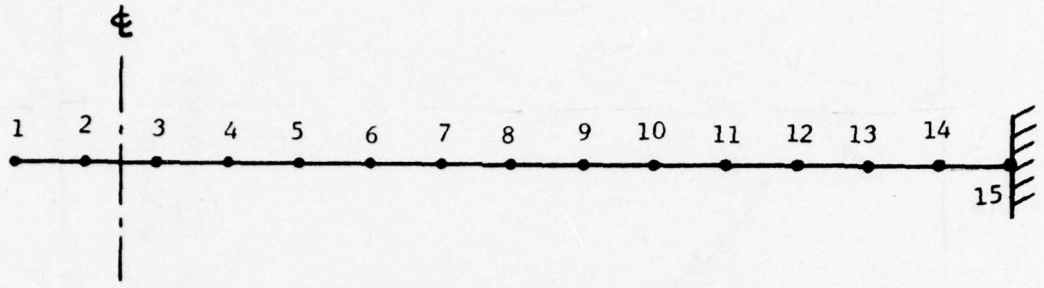

Fig. 12 Finite difference mesh along radial direction for a clamped axisymmetric spherical cap ($\lambda = 5$).

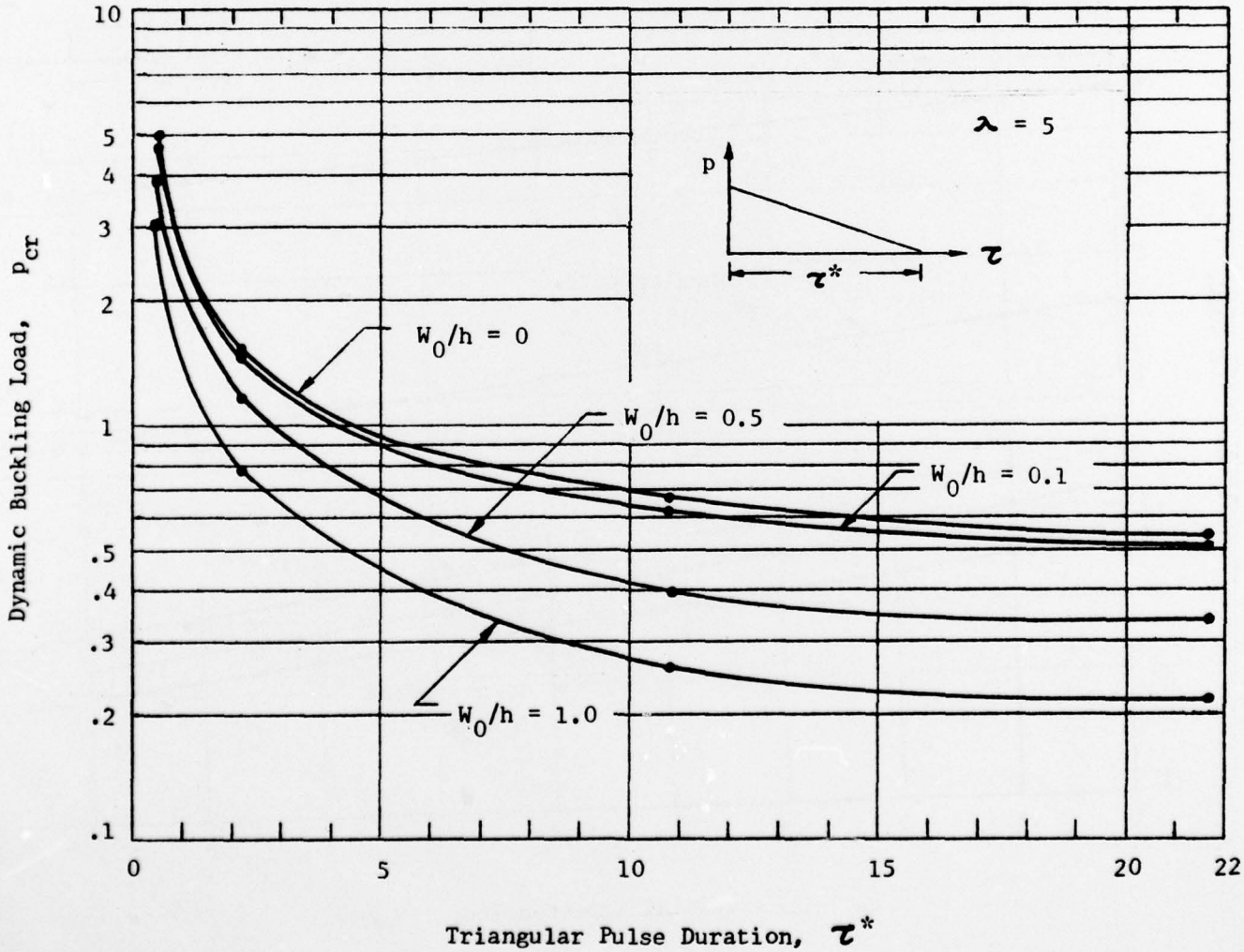

Fig. 13 Dynamic buckling load vs triangular pulse duration for an axisymmetric spherical cap ($\lambda = 5$) with initial imperfection.

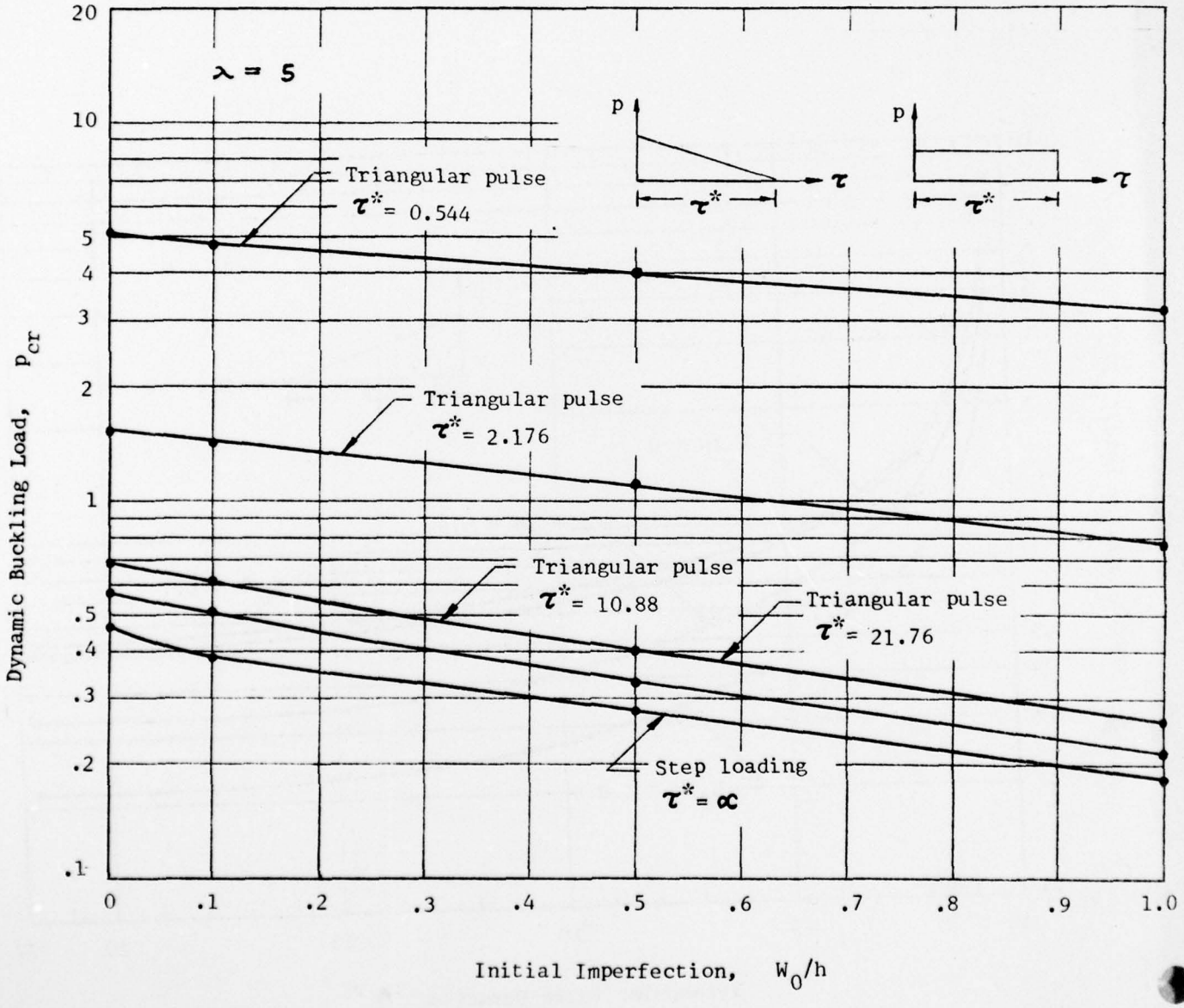

Fig. 14 Dynamic buckling load vs initial imperfection for an axisymmetric spherical cap ($\lambda = 5$).

SECURITY CLASSIFICATION OF THIS PAGE (When Data Entered)

REPORT DOCUMENTATION PAGE		READ INSTRUCTIONS BEFORE COMPLETING FORM
1. REPORT NUMBER	2. GOVT ACCESSION NO.	3. RECIPIENT'S CATALOG NUMBER
4. TITLE (and Subtitle) DYNAMIC BUCKLING OF AXISYMMETRIC SPHERICAL CAPS WITH INITIAL IMPERFECTIONS		5. TYPE OF REPORT & PERIOD COVERED 6. PERFORMING ORG. REPORT NUMBER
7. AUTHOR(s) Robert Kao and Nicholas Perrone		8. CONTRACT OR GRANT NUMBER(s) NAVYN00014-75-C-0946
9. PERFORMING ORGANIZATION NAME AND ADDRESS School of Engineering & Applied Science The George Washington University Washington, D. C. 20052		10. PROGRAM ELEMENT, PROJECT, TASK AREA & WORK UNIT NUMBERS
11. CONTROLLING OFFICE NAME AND ADDRESS Office of Naval Research Arlington, Virginia 22217		12. REPORT DATE December 1977 13. NUMBER OF PAGES 36
14. MONITORING AGENCY NAME & ADDRESS(if different from Controlling Office)		15. SECURITY CLASS. (of this report) UNCLASSIFIED 15a. DECLASSIFICATION/DOWNGRADING SCHEDULE

16. DISTRIBUTION STATEMENT (of this Report)

APPROVED FOR PUBLIC RELEASE: DISTRIBUTION UNLIMITED

17. DISTRIBUTION STATEMENT (of the abstract entered in Block 20, if different from Report)

18. SUPPLEMENTARY NOTES

19. KEY WORDS (Continue on reverse side if necessary and identify by block number)

Dynamic buckling	Initial imperfections
Step loading	Spherical cap
Triangular pulse	Finite differences
Dynamic snap-through	Nonlinear relaxation method
Inflection point method	Peak average displacement

20. ABSTRACT (Continue on reverse side if necessary and identify by block number)

Dynamic buckling loads are obtained for axisymmetric spherical caps with initial imperfections. Two types of loading are considered, namely, step loading of infinite duration and right triangular pulse. Results show that initial imperfections do indeed have the effect of reducing the buckling capacity for both dynamic and static reponses. Solutions also indicate that pulse duration has a very significant impact on the magnitude of the dynamic buckling load, and that the step loading of infinite duration is the limiting case of a triangular pulse and provides the most severe loading situation for dynamic analysis.

DD FORM 1 JAN 73 1473 EDITION OF 1 NOV 65 IS OBSOLETE
S/N 0102-014-6601

SECURITY CLASSIFICATION OF THIS PAGE (When Data Entered)